Title: The nuclei of human adult stem cells can move within the cell and generate cellular protrusions to contact other cells.

Authors: Carlos Bueno[1,*], David García-Bernal[1,2], Salvador Martínez[3], Miguel Blanquer[1] and José M. Moraleda[1].

[1]Medicine Department and Hematopoietic Transplant and Cellular Therapy Unit, Institute of Biomedical Research (IMIB), University of Murcia, Faculty of Medicine, Murcia, 30120, Spain.

[2]Biochemistry, Molecular Biology and Immunology Department, University of Murcia, Faculty of Medicine, Murcia, 30100, Spain

[3]Instituto de Neurociencias de Alicante (UMH-CSIC), Universidad Miguel Hernandez, San Juan, Alicante, 03550, Spain.

*Correspondence: Carlos Bueno, PhD., Medicine Department and Hematopoietic Transplant and Cellular Therapy Unit, Institute of Biomedical Research (IMIB), University of Murcia, Faculty of Medicine, Murcia, 30120, Spain. Tel.: 0034-968885013. Fax: 00-34-868884150. E-mail: carlos.bueno@um.es

Summary

Despite a considerable interest in understanding the mechanisms regulating nucleus structure, chromatin organization and nuclear positioning over decades, the exact significance of the variety of morphologies and positioning that cell nuclei can adopt and their relationship in cellular function is still far from being clearly understood. In this study, we examined the functional significance of the variety of morphologies and positioning that cell nuclei of human bone marrow-derived mesenchymal stem cells can adopt during neural-like differentiation. Here, we show that after neural induction, human bone marrow-derived mesenchymal stem cells an intermediate cellular state in which the nuclei are observed to be able to move within the cells, switching shapes and positioning and even generating cellular protrusions as they attempt to contact the cells around them. These findings suggest that changes in nuclear positioning are due to the fact that human cell nuclei are somehow sensing their surroundings.

Highlights

- During neural-like differentiation hBM-MSCs pass through a intermediate stage.
- During the intermediate stage, cell nuclei move and generate cellular protusions.
- Contacts occur between the cell nuclei of hBM-MSC-derived intermediate cells.
- During the intermediate stage, human cell nuclei are somehow sensing their surroundings.

eTOC blurb

Bueno et al. report that during neural-like differentiation, hBM-MSCs pass through a intermediate cellular stage in which the cell nuclei are able to move within the cells switching shapes and positioning and even generating cellular protrusions as they attempt to contact other cells. These findings indicate that during the intermediate stage, the human cell nuclei are somehow sensing their surroundings.

Introduction

Since the first observation of a nucleus in 1700 (Osorio et al., 2013), our knowledge of nuclear composition, organization, and positioning has continuously evolved (Gundersen and Worman., 2013; Skinner and Johnson., 2017; Misteli et al., 2020). Most textbooks depict the nucleus as a spherical or ovoid object at the center of the cell. However, different cell types have very different nuclear shapes and the position of nuclei varies dramatically from this simple view (Gundersen and Worman., 2013; Jevtić et al., 2014; Skinner and Johnson., 2017). Although the cell nucleus has always been considered as the largest and most rigid organelle of eukaryotic cells, emerging views of the nucleus indicate a more dynamic organelle than expected (Kalukula et al., 2022).

There is increasing evidence that nuclei are frequently asymmetrically positioned depending on cell type, developmental stage, migratory state, and differentiation status (Dupin and Etienne-Manneville., 2011; Gundersen and Worman., 2013; Calero-Cuenca et al., 2018; Almonacid et al., 2019; Deshpande et al., 2021). It has been reported that the position of the nucleus contributes to cell mechanics, as gene regulation through relative genome segregation and the organization of cells within tissues (Gundersen and Worman., 2013; Bone and Starr., 2016; Almonacid et al., 2019; Deshpande et al., 2021). Furthermore, it is important to note that changes in nuclear morphology and positioning are often associated with cellular dysfunction and disease (Zwerger et al., 2011; Gundersen and Worman., 2013; Manda et al., 2023). Therefore, the nucleus must be considered not only as the primary site for the storage of genetic material and gene transcription but also as a fundamental mechanical component of the cellular structure (Kalukula et al., 2022). Despite these advances, the exact significance of nuclear positioning in cellular function and tissue physiology is still far from being clearly understood (Dupin and Etienne-Manneville., 2011; Gundersen and Worman., 2013; Jevtić et al., 2014).

In our laboratory we focus on the differentiation of human mesenchymal stem cells (hMSCs) to generate a neuronal lineage (Bueno et al., 2013; Bueno et al., 2019; Bueno et al., 2021a; Bueno et al., 2021b; Bueno et al., 2022). hMSCs are considered as promising candidates for cell-based regenerative medicine due to their self-renewal capacity, multilineage differentiation potential,

trophic effects and immunomodulatory properties (Pittenger et al., 2019; García-Bernal et al., 2021). Controlled neural differentiation of hMSCs could therefore become an important source of cells for cell therapy of neurodegenerative diseases, as autologous adult hMSCs are easily harvested and effectively expanded (Mollinari et al., 2018; Choudhary et al., 2020; Hernández et al., 2020).

Over the past two decades, it has been reported that bone marrow-derived cells (BMDCs) and hMSCs can be induced to overcome their mesenchymal fate and differentiate into neural cells, both in vitro (Woodbury et al., 2000; Woodbury et al., 2002; Muñoz-Elias et al., 2003; Jeong et al., 2004; Suon et al., 2004; Hermann et al., 2006; Ning et al., 2006; Azedi et al., 2017; Radhakrishnan et al., 2019) and in vivo (Azizi et al., 1998; Kopen et al., 1999; Brazelton et al., 2000; Mezey et al., 2000; Priller et al., 2001; Mezey et al., 2003; Muñoz-Elias et al., 2004), a phenomenon known as transdifferentiation. The term transdifferentiation refers to the conversion of one mature cell type into another cell of different blastodermic origin (Jopling et al., 2011; Merrell and Stanger., 2016). Such interconversions may involve to regress into an intermediate step before cells differentiate into a new blastodermic potentiality and mature phenotype, or they may occur directly in a process that bypasses such intermediate phenotypes (Jopling et al., 2011; Merrell and Stanger., 2016). The actual occurrence of neuronal transdifferentiation of BMDCs and MSCs is currently much debated because the findings and their interpretation have been questioned (Lu et al., 2004; Kemp et al., 2014). The main argument against these observations in culture studies is that MSCs rapidly adopt neural-like morphologies by retraction of the cytoplasm, rather than by active neurite extension (Lu et al., 2004; Neuhuber et al., 2004; Bertani et al., 2005; Krabbe et al., 2005). The in vivo neural transdifferentiation of BMDCs and hMSCs has also been questioned, as cell fusion could explain the development of new cell types, that are misinterpreted as transdifferentiated cells (Kemp et al., 2014).

In a previous publication (Bueno et al., 2022), we showed that when human bone marrow-derived MSCs (hBM-MSCs) were exposed to a neural induction medium, they rapidly reshaped from a flat to a spherical morphology. Subsequently, hBM-MSCs could maintain the spherical

morphology or adopt a new one; they gradually adopted a neural-like morphology through active neurite extension or re-differentiated back to the mesenchymal fate. Furthermore, we found that hBM-MSCs can rapidly and repeatedly switch lineage without cell division. Our results provide evidence that differentiation of hBM-MSCs into neural-like cells requires a transition through a transient and characterized intermediate state of hBM-MSCs (hBM-MSC-derived intermediate cells) and provide a stronger basis for rejecting the idea that the rapid acquisition of a neural-like morphology during MSC transdifferentiation is merely an artifact.

This previous work also highlights that nuclear remodeling occurs during in vitro neural-like differentiation of hBM-MSCs. We found that nuclei in hBM-MSC-derived intermediate cells moved within the cell, adopting different morphologies, and even forming two nuclei connected by an internuclear bridge. These nuclear movements generated cellular protrusions that appeared and disappeared from the surface of hBM-MSC-derived intermediate cells. The hBM-MSC-derived intermediate cells positioned their nucleus at the front of the cell during migration. Our results showed that binucleated hBM-MSCs can be formed during neural-like differentiation with independence of any cell fusion, providing evidence that transdifferentiation may also be the mechanism behind the presence of gene-marked binucleated neurons after gene-marked bone marrow-derived cell transplantation. It is important to note that binucleated and polymorphic nuclear cells have been detected in adult neurogenic niches (Doetsch et al., 1997; Wittmann et al., 2009; Guerrero-Cázares et al., 2011; Cebrián-Silla et al., 2017; Bueno et al., 2019).

Taken together, these findings suggest that to date there is no conclusive evidence to continue to consider neuronal transdifferentiation of BMDCs and MSCs as a simple experimental artifact, since it recapitulates some structural steps described in vivo (Jopling et al., 2011; Merrell and Stanger., 2016). Therefore, future studies are needed to understand the mechanisms of these cell conversion processes and eventually harness them for use in regenerative medicine.

In the present study, we investigated the sequence of biological events during neural-like differentiation of hBM-MSCs using live-cell nuclear fluorescence labelling and time-lapse

microscopy to understand why the nuclei of hBM-MSC-derived intermediate cells move within the cell generating the cellular protrusions that appear and disappear from the surface.

Results

Characterization of hBM-MSCs cultures

In a previous publication (Bueno et al., 2022), we showed that hBM-MSCs did not express hematopoietic lineage markers such as CD45, CD14, CD34 and CD20, and were positive for CD90, CD105, CD73, thereby demonstrating a characteristic immunophenotype of hMSCs. Under proliferation conditions, hBM-MSCs displayed a flat, fibroblast-like morphology with β-III-tubulin microtubules and actin microfilaments oriented parallel to the longitudinal axis of the cell (Fig. 1A). During interphase, hBM-MSCs displayed a flattened, ellipsoidal nucleus, often located in the center of the cell and with a nuclear volume of approximately 419′30 ± 106′38 μm3 (Fig. 1B). The dynamic localization of the nuclear lamina was analyzed by immunostaining for lamin A/C, a nuclear lamina component (De Leeuw et al., 2018) and the dynamic localization of the nucleoli was analyzed by immunostaining for fibrillarin, the main component of the active transcription centers (Ochs et al., 1985). A speckled pattern was observed distributed throughout the nucleus with heterogeneity in the number, size, and distribution of the fibrillarin positive specks (Fig. 1C). Laser scanning confocal microscopy revealed that the inner surface of the nuclear envelope is lined by the nuclear lamina (Fig. 1D).

Characterization of hBM-MSC-derived intermediate cells

As mentioned above, we showed that following neural induction, hBM-MSCs rapidly reshaped from a flat to a spherical morphology (hBM-MSCs intermediate cells). Subsequently, we observed that hBM-MSC-derived intermediate cells can preserve their spherical shape, change to that of neural-like cells through active neurite extension or revert back to their mesenchymal morphology. In this study, we focus on hBM-MSC-derived intermediate cells that can maintain their spherical shape for several days without assuming new fates. To better understand why the

nuclei of hBM-MSC-derived intermediate cells move within the cell to generate the cellular protrusions, we performed time-lapse microscopy and immunocytochemical analyses of histone H2B-GFP transfected hBM-MSCs within the first 70 hours of neural induction. The time-lapse experiments were performed using a higher magnification objective and a shorter image capture interval than previously published experiments (Bueno et al., 2022).

Time-lapse imaging revealed that when hBM-MSCs were exposed to a neural induction medium, they rapidly reshaped from a flat to a spherical morphology (Fig. 2A and Supplementary Video S1). We then observed hBM-MSC-derived intermediate cells in which nuclear movements generated only one cell protrusion (Fig. 2A, white arrow and Supplementary Video S1) and hBM-MSC-derived intermediate cells in which nuclear movements alternately generated one or two cellular protrusions (Fig. 2A, yellow arrows and Supplementary Video S1). We found that when hBM-MSC-derived intermediate cell has a nucleus without lobes, its movement within the cell generates only one cell protrusion (Fig. 2B and Supplementary Video S2). However, if the hBM-MSC-derived intermediate cell has a lobed nucleus it will generate one or two cellular protrusions depending on how it moves within the cell (Fig. 2C).

Although the cell nuclei switch their morphologies while moving, time-lapse imaging and immunocytochemical analysis revealed that hBM-MSC-derived intermediate cells have three main different nuclear morphologies: Tail-less nuclei (Fig. 3A, white asterisk), tailed nuclei (Fig. 3A, green asterisk) and lobed nuclei (Fig. 3A, yellow asterisk). Tail-less and tailed nuclei movements generate only a single cell protrusion (Fig. 3A, white and green arrows respectively). However, as mentioned above, lobed nucleus movements generate one or two cellular protrusions depending on how it moves within the cell (Fig. 3A, yellow arrows).

Confocal microscopy analysis and 3D reconstruction revealed that there are small variations in both shape and size within the three types of nuclear morphology (Fig. 3B). Tail-less nuclei, tailed nuclei and lobed nuclei have a volume of approximately 327′11 ± 94′19 μm3, 306′89 ± 16′50 μm3 and 361′75 ± 147′44 μm3 respectively. It is important to note that confocal microscopic analysis

and 3D reconstruction also revealed that the lobes of the lobed nuclei can be located in different z-planes (Fig. 3C).

We observed that tail-less nuclei and tailed nuclei contained one or two fibrillarin positive specks, whereas lobed nuclei contained one or two fibrillarin positive specks in each lobe (Fig. 3D). No positive fibrillarin specks have been detected either in the tail of the tailed nuclei or in the region of nucleoplasm connecting each lobe of lobed nuclei. Laser scanning confocal microscopy also revealed that the inner surface of the nuclear envelope is lined by the nuclear lamina (Fig. 3E).

Confocal microscopy analysis of the cytoskeletal organization of hBM-MSC-derived intermediate cells showed that the cytoskeletal network is reorganized. Actin microfilaments and β-III tubulin microtubules are no longer oriented parallel to the longitudinal axis of the hBM-MSC-derived intermediate cells (Fig. 4A). Furthermore, confocal microscopy analysis and 3D reconstruction revealed that cell protrusions are almost devoid of actin microfilaments and that the β-III tubulin protein is concentrated at the cell protrusion rim (Fig. 4B, black arrows). Although it has been reported that direct connections between the actin cytoskeleton and the nucleus govern nuclear positioning and nuclear movement during cell polarization and migration (Dupin and Etienne-Manneville, 2011; Gundersen and Worman, 2013; Calero-Cuenca et al., 2018), we observed that the absence of the cytoskeletal network could facilitate nuclear movement within the cell. Future research is required to determine the feasibility of this conjecture.

Nuclear remodeling

To further understand how the three different types of nuclei that move within the hBM-MSC-derived intermediate cells are formed, we examined the sequence of biological events during neural-like differentiation of histone H2B-GFP-transfected hBM-MSCs using time-lapse microscopy. Time-lapse imaging revealed that there are variations in the form and time at which cell nuclei adopt these different nuclear morphologies (Supplementary Videos S3-S11). Although future studies are needed to determine all the possible different nuclear remodeling sequences that

occur when hBM-MSCs reshape from a flat to a spherical morphology, below we have described some examples of the formation of each of the three types of nuclei that move within hBM-MSC-derived intermediate cells.

We observed that tail-less nuclei are formed by a single nuclear remodeling that occurs as the cell reshapes from a flat to a spherical morphology, positioning the nucleus in a peripheral position within the cell (Fig. 5, white arrows and Supplementary Videos S3 and S4). The duration of this particular process is approximately 30 hours. Subsequently, the tail-less nucleus began to move within the hBM-MSC-derived intermediate cells. (Fig. 5, yellow arrows and Supplementary Videos S3 and S4).

Time-lapse images also showed that tailed nuclei are formed by one (Supplementary Video S5) or two nuclear remodeling sequences. Below, we show an example of the formation of a tailed nucleus generated by two nuclear remodeling sequences (Fig. 6 and Supplementary Videos S6 and S7). We found that first a nuclear remodeling sequence occurs as the cell reshapes from a flat to a spherical morphology, positioning the nucleus in a peripheral position within the cell (Fig. 6, white arrows and Supplementary Videos S6 and S7). The duration of this particular process is approximately 12 hours. Subsequently, the cell nucleus moves (Fig. 6, green arrows and Supplementary Videos S6 and S7) and undergoes a second nuclear remodeling sequence in which a tailed process in the nucleus is formed (Fig. 6, yellow arrows and Supplementary Videos S6 and S7). The duration of this particular process is approximately 5 hours. Finally, the tailed nucleus began to move within the hBM-MSC-derived intermediate cells. (Fig. 6, green arrows and Supplementary Videos S6 and S7). Time-lapse imaging also revealed that as the tailed nuclei move within the cell, the tails can switch shape and size (Fig. 7A and Supplementary Video S8) and even appear to move in different z-planes (Fig. 7B and Supplementary Videos S6 and S7). Future analyses will be needed to determine whether the nuclei use the tails to stabilize their position within the cell.

Time-lapse imaging also revealed that lobed nuclei are formed by one (Supplementary Video S8) or two nuclear remodeling sequences. Below, we show you an example of the formation of a

lobed nucleus generated by two nuclear remodeling sequences (Fig. 8 and Supplementary Videos S9 and S10). We found that first a nuclear remodeling sequence occurs as the cell reshapes from a flat to a spherical morphology, positioning the nucleus in a peripheral position within the cell (Fig. 8, white arrows and Supplementary Videos S9 and S10). The duration of this particular process is approximately 14 hours. Subsequently, the cell nucleus moves (Fig. 8, green arrows and Supplementary Videos S9 and S10) and undergoes a second nuclear remodeling sequence in which a lobed nucleus is formed (Fig. 8, yellow arrows and Supplementary Videos S9 and S10). The duration of this particular process is approximately 5 hours. The lobed nuclei then began to move within the hBM-MSC-derived intermediate cells (Fig. 8, green arrows and Supplementary Videos S9 and S10). Finally, we also found that lobed nuclei can switch shape while moving within the cell, becoming tailed nuclei (Fig. 9, blue arrows and Supplementary Videos S9 and S10).

As mentioned above, confocal microscopy analysis and 3D reconstruction revealed that the lobes of the lobed nuclei can be located in different z-planes (Fig. 3C). This result together with the time-lapse noted in Figure 2A and Supplementary Video S1 suggest that each lobule of the lobed nuclei can move in different z-planes.

Quantitative analysis of time-lapse imaging revealed that the nuclear speed oscillated between 0.1 and 1.3 μm/min, with an average speed of 0,66 ± 0,45 μm/min. These findings are consistent with previous studies that reported the physical characteristics of typical nuclear movement in different cell types (Gundersen and Worman., 2013). Nuclear movement can generate cellular protrusions that extend up to a length similar to the cell diameter (Figure 2 and 4, and Supplementary Videos S1 and S2).

The hBM-MSC-derived intermediate cells use their cell nuclei to interact with other cells

Time-lapse imaging revealed that hBM-MSC-derived intermediate cell nuclei move within the cell, generating cellular protrusions as cell migration breakthrough process to contact surrounding cells (Figure 2, 5 and 8 and Supplementary Videos S1,S2,S4,S10). Furthermore, we observed that

contacts occur between cell nuclei of hBM-MSC-derived intermediate cells, even for several hours (Fig. 9 and Supplementary Video S11). Confocal microscopy analysis (Fig. 10A) and 3D reconstruction (Fig. 10B) revealed that tail-less nuclei, tailed nuclei and lobed nuclei contact each other. We note that lobed nuclei can contact other cells through one lobe or both simultaneously or successively (Fig. 2A and Supplementary Video S1).

Taken together, these findings suggest that changes in nuclear positioning are due to the fact that cell nuclei are somehow sensing their surroundings.

Discussion

The fate of adult cells was thought to be restricted to their tissue blastodermic of origin (Waddington., 1957). However, there is now a large body of evidence suggesting that under physiological conditions and certain experimental conditions, adult stem cells may be more plastic than we previously thought in that they can become cells of unrelated lineages, a phenomenon known as transdifferentiation (Raff., 2003; Jopling et al., 2011; Merrell and Stanger., 2016; Rajagopal and Stanger., 2016). In this process, cells pass through intermediate states that are not well understood (Jopling et al., 2011; Reid and Tursun., 2018). Given the potential application of this cell conversion process in regenerative medicine and disease modeling, a better understanding of intermediate states is crucial to avoid uncontrolled conversion or proliferation, which poses a risk to patients (Jopling et al., 2011; Eguizabal et al., 2013; Reid and Tursun., 2018).

Over the last two decades, it has been reported that BMDCs and hMSCs can be induced to overcome their mesenchymal fate and differentiate into neural cells, both in vitro (Woodbury et al., 2000; Woodbury et al., 2002; Muñoz-Elias et al., 2003; Jeong et al., 2004; Suon et al., 2004; Hermann et al., 2006; Ning et al., 2006; Azedi et al., 2017; Radhakrishnan et al., 2019) and in vivo (Azizi et al., 1998; Kopen et al., 1999; Brazelton et al., 2000; Mezey et al., 2000; Priller et al., 2001; Mezey et al., 2003; Muñoz-Elias et al., 2004). However, the neuronal transdifferentiation of BMDCs and MSCs is still considered to be merely an artefact (Lu et al.,

2004; Krabbe et al., 2005; Kemp et al., 2014). The main argument against these observations in culture studies is that MSCs rapidly adopt neuronal-like morphologies by retraction of the cytoplasm, rather than by active neurite extension (Lu et al., 2004; Neuhuber et al., 2004; Bertani et al., 2005, Krabbe et al., 2005). The main argument against neuronal transdifferentiation of BMDCs and hMSCs in vivo is that cell fusion could explain the development of new cell types, that are misinterpreted as transdifferentiated cells (Kemp et al., 2014).

In previous publications, we have shown that MSCs isolated from adult human tissues can differentiate into neural-like cells, both in vitro and in vivo (Bueno et al., 2013; Bueno et al., 2019; Bueno et al., 2021a; Bueno et al., 2021b; Bueno et al., 2022). We found that when hBM-MSCs were exposed to a neural induction medium, they rapidly reshaped from a flat to a spherical morphology, Subsequently, hBM-MSCs could maintain the spherical morphology or adopt a new one; they gradually adopted a neural-like morphology through active neurite extension or re-differentiated back to the mesenchymal fate. Furthermore, we found that hBM-MSCs can rapidly and repeatedly switch lineage without cell division. These results provide evidence that the differentiation of hBM-MSCs into neural-like cells requires a transition through an intermediate state, as described in the natural transdifferentiation processes (Jopling et al., 2011; Eguizabal et al., 2013; Merrell and Stanger, 2016; Reid and Tursun., 2018).

This previous work also highlights that nuclear remodeling occurs during in vitro neural-like differentiation of hBM-MSCs. We found that nuclei in hBM-MSC-derived intermediate cells moved within the cell, adopting different morphologies and even forming two nuclei connected by an internuclear bridge, independently of any cell fusion. These results provide a strong basis for rejecting the idea that the rapid acquisition of a neural-like morphology during in vitro MSC transdifferentiation is merely an artefact and also provide evidence that transdifferentiation may also be the mechanism behind the presence of gene-marked binucleated neurons after gene-marked bone marrow-derived cell transplantation.

It is important to note that the studies describing the presence of binucleated Purkinje neurons after bone marrow-derived cell transplantation suggest, but do not conclusively demonstrate, that

cell fusion is the underlying mechanism to explain the presence of binucleated neurons (Alvarez-Dolado et al., 2003; Weimann et al., 2003). Futhermore, it has been reported that binucleated Purkinje neurons are also present in healthy, unmanipulated mice and humans (Magrassi et al., 2007; Kemp et al., 2014). In addition, many authors have described binucleated neurons in various central and peripheral parts of the nervous system (Altman., 1963; Das., 1967; Ribak and Seress., 1983; Portiansky et al., 2006). In addition, many authors have reported that many cultured hippocampal neurons (Wittmann et al., 2009; their Fig. S2), and neural stem cells located in the ventricular-subventricular zone of the anterolateral ventricular wall of the human fetal brain (Guerrero-Cázares et al., 2011; their Fig. 2C) and adult mouse brain (Cebrián-Silla et al., 2017; their Figs. 1E, 4I, 6F, S1B, S2B and S6A and Doetsch et al., 1997; their Fig. 3A) have two nuclei connected by an internuclear bridge. Taken together, these results suggest that to date there is no conclusive evidence to date to continue to consider the neuronal transdifferentiation of BMDCs and hMSCs as an artefact. 2

Therefore, future studies are needed to optimize the various neural induction protocols that have been developed for MSCs (Jimenez-Acosta et al., 2022), not only to understand the mechanisms of these cellular conversion processes, but also to eventually harness them for use in regenerative medicine (Jopling et al., 02011; Eguizabal et al., 2013; Mollinari et al., 2018). Our current research aims to improve our understanding of what hBM-MSCs look like at this intermediate stage. We wanted to know why the nuclei of hBM-MSC-derived intermediate cells move within the cell and generate the cellular protrusions that appear and disappear from the surface.

In this study, we have shown that once the hBM-MSCs enter this intermediate stage, the cell nuclei begin to move within the cell and generate the cellular protrusions as they try to contact the surrounding cells. It is important to note that interkinetic nuclear migration in neural progenitors underlay normal neurogenesis during normal development (Kosodo., 2012; Spear and Erickson., 2012), suggesting that the observed nuclear motility in hBM-MS-derived intermediated cells recapitulates an intermediate stage before to decide proliferative of

differentiative progression in development and transdifferentiation. Future research is required to determine the feasibility of this conjecture.

We also found that contacts occur between the cell nuclei of hBM-MSC-derived intermediate cells, even for several hours. These findings suggest that changes in nuclear positioning occur because cell nuclei somehow sense their surroundings. Under our knowledge, we have described for the first time the process of direct interactions between cells nuclei, which opens the possibility of a new level of intercellular interaction. During this intermediate phase, nuclear factors may be interchanged by neighboring cells and directly modify transcriptomes. Extensive studies are required to determine the mechanisms and consequences of this process of direct interactions between cells nuclei in normal and pathologic circumstances.

This work also highlights that cell nuclei moving within hBM-MSC intermediate cells have mainly three different morphologies: tail-less nuclei, tailed nuclei, and lobed nuclei. We have shown that there are variations in the shape and time at which the nuclei of hBM-MSC adopt the different nuclear morphologies observed in hBM-MSC-derived intermediate cells. We also found that tail-less and tailed nuclei movements generate only a single cell protrusion when attempting to contact other cells. However, lobed nuclei movements generate one or two cellular protrusions depending on how it moves within the cell. Lobed nuclei may contact other cells through one lobe or both simultaneously or successively. Nevertheless, it is important to note that the three different nuclear morphologies observed in hBM-MSC intermediate cells can be interchanged as the nucleus moves within the cell.

Although future experiments will be needed to understand why there are different nuclear morphologies in hBM-MSC-derived intermediate cells and why they are formed in different ways, our results demonstrate that the nucleus should already be considered not only as the primary site for the storage of genetic material and the transcription of genes, but also as a fundamental mechanical component of the cell.

It is important to note that, beyond the central nervous system, the presence of lobed nuclei has been reported in most immune cells (Hoffmann et al., 2007; Skinner and Johnson., 2017) and in various human organs, including the heart and liver (Kachi and French., 1994; Paradis et al., 2014). However, the functional significance of multilobed nuclear structures is not yet known (Kachi and French., 1994; Hoffmann et al., 2007; Paradis et al., 2014; Skinner and Johnson., 2017). It would therefore be interesting to investigate whether these nuclear structures are also associated with nuclear movement within the cell.

In summary, hBMSCs could not only help to increase our understanding of the mechanisms underlying cellular plasticity, and eventually harness them for use in regenerative medicine, but also facilitate an understanding of the mechanisms regulating nuclear structure and dynamics.

Methods

Ethical conduct of research

The authors declare that all protocols used to obtain and process all human samples were approved by the local ethics committees of the Miguel Hernández University of Elche (No. UMH.IN.SM.03.16) and University of Murcia (HULP3617.05/07/2012; HUSA19/1531.17/02/2020) according to Spanish and European legislation and conformed to the ethical guidelines of the Helsinki Declaration. Donors provided written informed consent before obtaining samples.

Isolation and culture of hBM-MSCs

A standard protocol for isolation and expansion of MSCs was used as previously described (Bueno et al., 2022). Bone marrow aspirates were obtained by percutaneous direct aspiration from the iliac crest of 5 healthy volunteers at University Hospital Virgen de la Arrixaca (Murcia, Spain). Bone marrow was collected with 20 U/ml sodium heparin, followed by a Ficoll density gradient-based separation by centrifugation at 540g for 20 min. After, mononuclear cell fraction

was collected, washed twice with Ca^{2+}/Mg^{2+}-free phosphate buffered saline (PBS) (Gibco Invitrogen) and seeded into 175-cm2 culture flasks (Nunc, Thermo Fisher Scientific) at a cell density $1.5x10^5$ cells/cm^2 in serum-containing media (designated as the basal media), composed of DMEM low glucose medium (Thermo Fisher Scientific) supplemented with 10% fetal bovine serum (FBS; Lonza), 1% GlutaMAX (Thermo Fisher Scientific), non-essential amino acid solution (Sigma-Aldrich) and 1% penicillin/streptomycin (Thermo Fisher Scientific). After 3 days of culture at 37ºC and 7% CO_2, non-attached cells were removed and fresh complete medium was added. Culture media were renewed every 2 days, and the isolated hBMSCs were passaged when cultures were 70-80% confluent. All studies were performed using hBMSCs expanded within culture passages 3-4.

Expression Vectors and Cell Transfection

The expression vectors used in the present study were H2B-eGFP, a gift from Geoff Wahl (Addgene plasmid # 11680; http://n2t.net/addgene:11680; RRID:Addgene_11680; Kanda et al., 1998). A standard protocol for transfecting MSCs was used as previously described (Bueno et al., 2022). Isolated hBMSCs-derived cells were transfected using the Gene Pulser-II Electroporation System (Bio-Rad Laboratories). Electroporation was performed in a sterile cuvette with a 0.4-cm electrode gap (Bio-Rad Laboratories), using a single pulse of 270 V, 500 µF. Plasmid DNA (5 µg) was added to 1.5×10^6 viable hBMSCs-derived cells in 0.2-ml DMEM low glucose medium (Thermo Fisher Scientific) before electrical pulsing.

Time-lapse microscopy of histone H2B-GFP expressing hBM-MSCs cultured in neural induction media.

We used µ-Dish 35 mm, high Grid- 500 (Ibidi) for live cell imaging. Histone H2B-GFP transfected hBM-MSCs were plated onto collagen IV (Sigma-Aldrich) coated plastic or glass coverslips. To induce neural differentiation, cells at passage 3–4 were allowed to adhere to the plates overnight. Basal media was removed the following day and the cells were cultured for 2 days in serum-free media (designated as the neural basal media) consisting in Dulbecco's

modified Eagle's medium/F12 (DMEM/F12 Glutamax, Gibco) supplemented with N2-supplement (R&D systems), 0.6% glucose (Sigma-Aldrich), 5mM HEPES (Sigma-Aldrich), 0.5% human serum albumin (Sigma-Aldrich), 0.0002% heparin (Sigma-Aldrich), non-essential amino acid solution (Sigma-Aldrich) and 100 U/ml penicillin-streptomycin (Sigma-Aldrich). On day 3, cells were cultured in neural induction media, consisting in the neural basal media supplemented with 500nM retinoic acid (Sigma-Aldrich) and 1mM dibutyryl cAMP (Sigma-Aldrich). Time-lapse analysis was carried out using a Widefield Leica Thunder-TIRF imager microscope. We perform time-lapse microscopy within the first 70 hours after neural induction media was added directly to the cells. Time-lapse images were obtained with a 40X objective every 10 min. During imaging, cells were enclosed in a chamber maintained at 37°C under a humidified atmosphere of 5% CO2 in air. Data are representative of ten independent experiments.

Immunocytochemistry

A standard immunocytochemical protocol was used as previously described (Bueno et al., 2013; Bueno et al., 2019; Bueno et al., 2021; Bueno et al., 2022). Histone H2B-GFP transfected hBM-MSCs were plated onto collagen IV (Sigma-Aldrich) coated plastic or glass coverslips and maintained in neural induction media. Cells were rinsed with PBS and fixed in freshly prepared 4% paraformaldehyde (PFA; Sigma-Aldrich). Fixed cells were blocked for 2 h in PBS containing 10% normal horse serum (Gibco) and 0.25% Triton X-100 (Sigma) and incubated overnight at 4 °C with antibodies against β-III-tubulin (TUJ1; 1:500, Covance) in PBS containing 1% normal horse serum and 0.25% Triton X-100. On the next day, cells were rinsed and incubated with the secondary antibody conjugated with Alexa Fluor® 594 (anti-mouse; 1:500, Molecular Probes). Cell nuclei were counterstained with DAPI (0.2 mg/ml in PBS, Molecular Probes). Alexa Fluor 488® phalloidin (Molecular Probes) was used to selectively stains F-actin. Data are representative of ten independent experiments per condition.

Images and Data Analyses

Photograph of visible and fluorescent stained samples were carried out in a Widefield Leica Thunder-TIRF imager microscope equipped with a digital camera or in confocal laser scanning microscope Leica TCS-SP8. We used Leica Application Suite X and Imaris software for image analysis and Filmora Video Editor software for video editing. Photoshop software was used to improve the visibility of fluorescence images without altering the underlying data. Data are representative of ten independent experiments per condition and are expressed as mean ± SD.

References

1. Almonacid, M., Terret, M. E. & Verlhac, M. H. Nuclear positioning as an integrator of cell fate. Curr Opin Cell Biol. 56, 122-129 (2019).

2. Altman, J. Autoradiographic investigation of cell proliferation in the brains of rats and cats. Anat. Rec. 145, 573-591 (1963).

3. Alvarez-Dolado, M. et al. Fusion of bone-marrow-derived cells with Purkinje neurons, cardiomyocytes and hepatocytes. Nature. 425, 968-973 (2003).

4. Azedi, F. et al. Comparative capability of menstrual blood versus bone marrow derived stem cells in neural differentiation. Mol. Biol. Rep. 44, 169-182 (2017).

5. Azizi, A. S., Stokes, D., Augelli, B. J., DiGirolamo, C. & Prockop, D. J. Engraftment and migration of human bone marrow stromal cells implanted in the brains of albino rats-Similarities to astrocyte grafts. Proc. Natl. Acad. Sci. U.S.A. 95, 3908-3913 (1998).

6. Bertani, N., Malatesta, P., Volpi, G., Sonego, P. & Perris, R. Neurogenic potential of human mesenchymal stem cells revisited: Analysis by immunostaining, time-lapse video and microarray. J. Cell Sci. 118, 3925-3936 (2005).

7. Bone, C. R. & Starr, D. A. Nuclear migration events throughout development. J Cell Sci. 129, 1951-1961 (2016).

8. Brazelton, T. R., Rossi, F. M., Keshet, G. I. & Blau, H. M. From marrow to brain: Expression of neuronal phenotypes in adult mice. Science. 290, 1775-1779 (2000).

9. Bueno, C., Ramirez, C., Rodríguez-Lozano, F. J, Tabarés-Seisdedos, R., Rodenas, M., Moraleda, J. M., Jones, J. R. & Martinez, S. Human adult periodontal ligament-derived cells integrate and differentiate after implantation into the adult mammalian brain. Cell Transplant. 22, 2017-2028 (2013).

10. Bueno, C., Martínez-Morga, M. & Martínez, S. Non-proliferative neurogenesis in human periodontal ligament stem cells. Sci Rep. 2019 Dec 2;9(1):18038. doi: 10.1038/s41598-019-54745-3.

11. Bueno, C. & Martínez, S. Neurogenesis similarities in different human adult stem cells. Neural Regen Res. 2021a Jan;16(1):123-124. doi: 10.4103/1673-5374.286967.

12. Bueno, C., Martínez-Morga, M., García-Bernal, D., Moraleda, J. M. & Martínez, S. Differentiation of human adult-derived stem cells towards a neural lineage involves a dedifferentiation event prior to differentiation to neural phenotypes. Sci Rep. 2021b Jun 8;11(1):12034. doi: 10.1038/s41598-021-91566-9.

13. Bueno, C., Blanquer, M., García-Bernal, D., Martínez, S. & Moraleda, J. M. Binucleated human bone marrow-derived mesenchymal cells can be formed during neural-like differentiation with independence of any cell fusion events. Sci Rep. 2022 Nov 30;12(1):20615. doi: 10.1038/s41598-022-24996-8.

14. Calero-Cuenca, F. J., Janota, C. S. & Gomes, E. R. Dealing with the nucleus during cell migration. Curr Opin Cell Biol. 50, 35-41 (2018).

15. Cebrián-Silla, A. et al. Unique organization of the nuclear envelope in the post-natal quiescent neural stem cells. Stem Cell Rep. 9, 203–216 (2017).

16. Choudhary, P., Gupta, A. & Singh, S. Therapeutic advancement in neuronal transdifferentiation of mesenchymal stromal cells for neurological disorders. J. Mol. Neurosci. https:// doi. org/ 10. 1007/ s12031- 020- 01714-5 (2020).

17. Das, G. D. Binucleated neurons in the central nervous system of the laboratory animals. Experientia 33, 1179-1180 (1977).

18. De Leeuw, R., Gruenbaum, Y. & Medalia, O. Nuclear Lamins: Thin Filaments with Major Functions. Trends Cell Biol. 28, 34-45(2018).

19. Deshpande, O. & Telley, I. A. Nuclear positioning during development: Pushing, pulling and flowing. Semin Cell Dev Biol. 120,10-21(2021).

20. Doetsch, F., Garcia-verdugo, J. M. & Alvarez-buylla, A. Cellular composition and three-dimensional organization of the subventricular germinal zone in the adult mammalian brain. J. Neurosci. 17, 5046-5061 (1997).

21. Dupin, I. & Etienne-Manneville, S. Nuclear positioning: mechanisms and functions. Int. J. Biochem. Cell Biol. 43, 1698-1707 (2011).

22. Eguizabal, C., Montserrat, N., Veiga, A. & Izpisua-Belmonte, J. C. Dedifferentiation, transdifferentiation, and reprogramming: future directions in regenerative medicine. Semin Reprod Med. 31, 82-94 (2013).

23. García-Bernal, D. et al. The Current Status of Mesenchymal Stromal Cells: Controversies, Unresolved Issues and Some Promising Solutions to Improve Their Therapeutic Efficacy. Front Cell Dev Biol. 2021 Mar 16;9:650664. doi: 10.3389/fcell.2021.650664.

24. Guerrero-Cázares, H. et al. Cytoarchitecture of the lateral ganglionic eminence and rostral extension of the lateral ventricle in the human fetal brain. J. Comp. Neurol. 519, 1165-1180 (2011).

25. Gundersen, G. G. & Worman, H. J. Nuclear positioning. Cell. 152, 1376-1389 (2013).

26. Hermann, A. et al. Comparative analysis of neuroectodermal differentiation capacity of human bone marrow stromal cells using various conversion protocols. J. Neurosci. Res. 83, 1502-1514 (2006).

27. Hernández, R. et al. Differentiation of human mesenchymal stem cells towards neuronal lineage: clinical trials in nervous system disorders. Biomol. Ther. 28, 34-44 (2020).

28. Hoffmann, K., Sperling, K., Olins, A. L. & Olins, D. E. The granulocyte nucleus and lamin B receptor: Avoiding the ovoid. Chromosoma116, 227-235 (2007).

29. Jeong, J. A. et al. Rapid neural differentiation of human cord blood-derived mesenchymal stem cells. Neuroreport. 15, 1731-1734 (2004).

30. Jevtić, P, Edens L. J., Vuković, L. D. & Levy, D. L. Sizing and shaping the nucleus: mechanisms and significance. Curr Opin Cell Biol. 28, 16-27 (2014).

31. Jimenez-Acosta, M. A., Hernandez, L. J. R., Cristerna, M. L. P., Tapia-Ramirez, J. & Meraz-Rios, M. A. Review: Neuronal differentiation protocols of mesenchymal stem cells. Adv. Biosci. Biotechnol. 13, 15-71 (2022).

32. Jopling, C., Boue, S., & Izpisua Belmonte J. C. Dedifferentiation, transdifferentiation and reprogramming: three routes to regeneration. Nat. Rev. Mol. Cell Biol. **12**, 79-89 (2011).

33. Kachi, K. & French, S. W. The connection between the nuclei of binucleated hepatocytes: An ultrastructural study. J. Submicrosc. Cytol. Pathol. 26, 163–172 (1994).

34. Kalukula Y, Stephens AD, Lammerding J, Gabriele S. Mechanics and functional consequences of nuclear deformations. Nat Rev Mol Cell Biol. 23, 583-602 (2022).

35. Kanda, T., Sullivan, K. F. & Wahl, G. M. Histone-GFP fusion protein enables sensitive analysis of chromosome dynamics in living mammalian cells. Curr. Biol. 8, 377-385 (1998).

36. Kemp, K., Wilkins, A. & Scolding, N. Cell fusion in the brain: Two cells forward, one cell back. Acta Neuropathol. 128, 629-638 (2014).

37. Kosodo Y. Interkinetic nuclear migration: beyond a hallmark of neurogenesis. Cell Mol Life Sci. 69, 2727-2738 (2012).

38. Kopen, G. C., Prockop, D. J. & Phinney, D. G. Marrow stromal cells migrate throughout forebrain and cerebellum, and they differentiate into astrocytes after injection into neonatal mouse brains. Proc. Natl. Acad. Sci. U.S.A. 96, 10711-10716 (1999).

39. Krabbe, C., Zimmer, J. & Meyer, M. Neural transdifferentiation of mesenchymal stem cells-A critical review. APMIS 113, 831-844 (2005).

40. Lu, P., Blesch, A. & Tuszynski, M. H. Induction of bone marrow stromal cells to neurons: differentiation, transdifferentiation, or artifact? J. Neurosci. Res. 77, 174-191 (2004).

41. Magrassi, L. et al. Induction and survival of binucleated Purkinje neurons by selective damage and aging. J. Neurosci. 27, 9885-9892 (2007).

42. Manda NK, Golla U, Sesham K, Desai P, Joshi S, Patel S, Nalla S, Kondam S, Singh L, Dewansh D, Manda H, Rokana N. Tuning between Nuclear Organization and Functionality in Health and Disease. Cells. 2023 Feb 23;12(5):706. doi: 10.3390/cells12050706.

43. Merrell, A. J. & Stanger, B. Z. Adult cell plasticity in vivo: de-differentiation and transdifferentiation are back in style. Nat. Rev. Mol. Cell Biol. 17, 413-25 (2016).

44. Mezey, E., Chandross, K. J., Harta, G., Maki, R. A. & McKercher, S. R. Turning blood into brain: Cells bearing neuronal antigens generated in vivo from bone marrow. Science 290, 1779-1782 (2000).

45. Mezey, E. et al. Transplanted bone marrow generates new neurons in human brains. Proc. Natl. Acad. Sci. U.S.A. 100, 1364-1369 (2003).

46. Misteli, T. The Self-Organizing Genome: Principles of Genome Architecture and Function. Cell. 183, 28-45 (2020).

47. Mollinari, C., Zhao, J., Lupacchini, L., Garaci, E., Merlo, D. & Pei, G. Transdifferentiation: a new promise for neurodegenerative diseases. Cell Death Dis. 2018 Aug 6;9(8):830. doi: 10.1038/s41419-018-0891-4.

48. Muñoz-Elias, G., Woodbury, D. & Black, I. B. Marrow stromal cells, mitosis and neuronal differentiation: stem cell and precursor functions. Stem Cells. 21,437-448 (2003).

49. Muñoz-Elias, G., Marcus, A. J., Coyne, T. M., Woodbury, D. & Black, I. B. Adult bone marrow stromal cells in the embryonic brain:Engraftment, migration, differentiation, differentiation, and long-term survival. J. Neurosci. 24, 4585-4595 (2004).

50. Neuhuber, B. et al. Reevaluation of in vitro differentiation protocols for bone marrow stromal cells: Disruption of actin cytoskeleton induces rapid morphological changes and mimics neuronal phenotype. J. Neurosci. Res. 77, 192-204 (2004).

51. Ning, H., Lin, G., Lue, T. F. & Lin, C. S. Neuron-like differentiation of adipose tissue-derived stromal cells and vascular smooth muscle cells. Differentiation. 74, 510-518 (2006).

52. Ochs, R. L., Lischwe, M. A., Spohn, W. H. & Busch, H. Fibrillarin: a new protein of the nucleolus identified by autoimmune sera. Biol. Cell. 54, 123-133 (1985).

53. Osorio, D. S. & Gomes, E. R. The contemporary nucleus: a trip down memory lane. Biol Cell. 105, 430-441(2013).

54. Paradis, A. N., Gay, M. S. & Zhang, L. Binucleation of cardiomyocytes: The transition from a proliferative to a terminally differentiated state. Drug Discov. Today 19, 602-609 (2014).

55. Pittenger, M. F., Discher, D. E., Péault, B. M., Phinney, D. G., Hare, J. M. & Caplan, A. I. Mesenchymal stem cell perspective: cell biology to clinical progress. NPJ Regen Med. 2019 Dec 2;4:22. doi: 10.1038/s41536-019-0083-6.

56. Portiansky, E. L., Barbeito, C. G., Flamini, M. A., Gimeno, E. J. & Goya, R. G. Presence of binucleate neurons in the spinal cord ofyoung and senile rats. Acta Neuropathol. 112, 647-649 (2006).

57. Priller, J. et al. Neogenesis of cerebellar Purkinje neurons from gene-marked bone marrow cells in vivo. J. Cell Biol. 155, 733-738 (2001).

58. Radhakrishnan, S. et al. In vitro transdifferentiation of human adipose tissue-derived stem cells to neural lineage cells - a stage-specific incidence. Adipocyte. 8, 164-177 (2019).

59. Raff, M. Adult stem cell plasticity: fact or artifact? Annu. Rev. Cell Dev. Biol. 19, 1-22 (2003).

60. Rajagopal, J. & Stanger, B. Z. Plasticity in the adult: How should the waddington diagram be applied to regenerating tissues?. Dev.Cell 36, 133-137 (2016).

61. Reid, A. & Tursun, B. Transdifferentiation: do transition states lie on the path of development? Curr. Opin. Syst. Biol. 11, 18-23 (2018).

62. Ribak, C. E. & Seress, L. Five types of basket cell in the hippocampal dentate gyrus: A combined Golgi and electron microscopic study. J. Neurocytol. 12, 577-597 (1983).

63. Skinner, B. M. & Johnson, E. E. Nuclear morphologies: their diversity and functional relevance. *Chromosoma*. **126**, 195-212 (2017).

64. Spear, P. C. & Erickson, C. A. Interkinetic nuclear migration: a mysterious process in search of a function. Dev Growth Differ. 54, 306-316 (2012).

65. Suon, S. et al. Transient differentiation of adult human bone marrow cells into neuron-like cells in culture: development of morphological and biochemical traits is mediated by different molecular mechanisms. Stem Cells Dev. 13, 625-635 (2004).

66. Waddington, C. H. The Strategy of the Genes. A Discussion of Some Aspects of Theoretical Biology (Allen & Unwin, 1957).

67. Weimann, J. M., Johansson, C. B., Trejo, A. & Blau, H. M. Stable reprogrammed heterokaryons form spontaneously in Purkinjeneurons after bone marrow transplant. Nat. Cell Biol. 5, 959-966 (2003).

68. Wittmann, M. et al. Synaptic activity induces dramatic changes in the geometry of the cell nucleus: Interplay between nuclear structure, histone H3 phosphorylation, and nuclear calcium signaling. J. Neurosci. 29, 14687-14700 (2009).

69. Woodbury, D., Schwarz, E. J., Prockop, D. J. & Black I. B. Adult rat and human bone marrow stromal stem cells differentiate into neurons. J. Neurosci. Res. 61, 364-370 (2000).

70. Woodbury, D., Reynolds, K. & Black, I. B. Adult bone marrow stromal stem cells express germline, ectodermal, endodermal, and mesodermal genes prior to neurogenesis. J. Neurosci. Res. 69, 908-917 (2002).

71. Zwerger, M., Ho, C. Y. & Lammerding, J. Nuclear mechanics in disease. Annu Rev Biomed Eng. 13, 397-428 (2011).

Acknowledgements: We greatly appreciate the technical assistance of Microscopy Section and the Tissue Culture Service of the University of Murcia.

Author contributions: C.B. conceived of the study, designed the study, carried out the molecular lab work and drafted the manuscript; D.G-B and M.B. designed experiments, participated in data analysis and helped draft the manuscript; S.M. and J.M.M. helped draft the manuscript and financial support.

Data availability statement: All data generated or analysed during this study are included in this published article (and its supplementary information files).

Competing interests: The authors declare no competing interests.

Funding: This study was supported by the Spanish Ministry of Science and Innovation, the Carlos III Health Institute (ISCIII), through The Spanish Network of Advanced Therapies (TERAV), projects RD21/0017/0001 and RD21/0017/0017, co-funded by European Union "NextGenerationEU. Plan de Recuperación Transformación y Resiliencia". It was also partially supported by Research Grant of the Universidad Católica San Antonio de Murcia (UCAM).

Figure legends

Figure 1. **Morphology of hBM-MSCs cultured in basal medium**. (A) Undifferentiated hBM-MSCs exhibited a fibroblast-like morphology with β-III tubulin microtubules and actin microfilaments oriented parallel to the longitudinal axis of the cell. (B) During interphase, hBM-MSCs displayed a flattened, ellipsoidal nucleus, often located in the center of the cell. (C) Distribution of fibrillarin-positive specks in the nuclei of undifferentiated hBM-MSCs. (D) Immunocytochemical analysis revealed that the inner surface of the nuclear envelope is lined by the nuclear lamina. Scale bar: 10 μm.

Figure 2. **Nuclear movement generated cellular protrusions that appeared and disappeared from the surface of hBM-MSC-derived intermediate cells**. (A) Time-lapse imaging showed that when hBM-MSCs were exposed to a neural induction medium, they rapidly reshaped from a flat to a spherical morphology. Subsequently, we observed hBM-MSC-derived intermediate cells (white asterisk) in which nuclear movements generate only one cell protrusion (white arrow), and hBM-MSC-derived intermediate cells (yellow asterisk) in which nuclear movements alternately generate one or two cellular protrusions (yellow arrows). (B) We found that when a hBM-MSC-derived intermediate cell has a nucleus without lobes, its movement within the cell generates only one cell protrusion (yellow arrow). (C) However, if the hBM-MSC-derived intermediate cell has a lobed nucleus it will generate one or two cellular protrusions depending on how it moves within the cell (yellow arrows). Scale bar: 10 μm. PhC: Phase-contrast photomicrographs.

Figure 3. **Characterization of hBM-MSC-derived intermediate cell nuclei**. (A) Immunocytochemical analysis revealed that hBM-MSC-derived intermediate cells primarily have three different nuclear morphologies: Tail-less nuclei (white asterisk), tailed nuclei (green asterisk) and lobed nuclei (yellow asterisk). Tail-less and tailed nuclei movements generate only one cell protrusion (white and green arrows respectively). However, lobed nuclei movements generate one or two cellular protrusions depending on how it moves within the cell (yellow arrows). Confocal microscopy analysis and 3D reconstruction revealed that there are small variations in both shape and size within the three types of nuclear morphology (B) and that the

lobes of the lobed nuclei can be located in different z-planes. (C) Immunocytochemical analysis revealed that tail-less nuclei and tailed nuclei contained one or two fibrillarin positive specks while lobed nuclei contained one or two fibrillarin-positive specks in each lobe. (D) The inner surface of the nuclear enveloped is lined by the nuclear lamina (E). Scale bar: 10 μm. PhC: Phase-contrast photomicrographs.

Figure 4. **Cytoskeletal organization of hBM-MSC-derived intermediate cells**. (A) Immunocytochemical analysis revealed that actin microfilaments and β-III tubulin microtubules are no longer oriented parallel to the longitudinal axis of the hBM-MSC-derived intermediate cells. (B) Confocal microscopy analysis and 3D reconstruction revealed that cell protrusions are almost devoid of actin microfilaments and that the β-III tubulin protein is concentrated at the cell protrusion rim (black arrows). Scale bar: 10 μm.

Figure 5. **Tail-less nuclei formation**. Time-lapse imaging revealed that tail-less nuclei are formed by a single nuclear remodeling that occurs as the cell reshapes from a flat to a spherical morphology, positioning the nucleus in a peripheral position within the cell (white arrows). Subsequently, the tail-less nucleus began to move within the hBM-MSC-derived intermediate cells (yellow arrows). Scale bar: 10 μm.

Figure 6. **Tailed nuclei formation by two nuclear remodeling sequences**. Time-lapse images show that first a nuclear remodeling sequence occurs as the cell reshapes from a flat to a spherical morphology, positioning the nucleus in a peripheral position within the cell (white arrows). Next, the cell nucleus moves (green arrows) and undergoes a second nuclear sequence in which a tailed nucleus is formed (yellow arrows). Finally, the tailed nucleus began to move within the hBM-MSC-derived intermediate cells (green arrows). Scale bar: 10 μm.

Figure 7. **The tails of the tailed nuclei can move within the hBM-MSC-derived intermediate cells, switching shape and size and even move in different z-planes**. (A) Time-lapse imaging revealed that as the tailed nuclei move within the cell, and the tails can switch shape and size

(yellow arrows). (B) Time-lapse images also showed that the tails even appear to move in different z-planes. Scale bar: 10 µm.

Figure 8. **Lobed nuclei formation by two nuclear remodeling sequences**. Time-lapse imaging showed that first a nuclear remodeling sequence occurs as the cell reshapes from a flat to a spherical morphology, positioning the nucleus in a peripheral position within the cell (white arrows). Subsequently, the cell nucleus moves (green arrows) and undergoes a second nuclear sequence in which a lobed nucleus is formed (yellow arrows). Afterwards, the lobed nuclei began to move within the hBM-MSC-derived intermediate cells (green arrows). Finally, we also noted that lobed nuclei can switch shape while moving within the cell, becoming tailed nuclei (blue arrows). Scale bar: 10 µm.

Figure 9. hBM-MSC-derived intermediate cells contact each other through their cell nuclei. Time-lapse imaging revealed that hBM-MSC-derived intermediate cell nuclei move within the cell generating cellular protrusions as they attempt to contact the cells around them, mainly observing contacts between the nuclei (green arrows). Scale bar: 10 µm.

Figure 10. **Tail-less nuclei, tailed nuclei and lobed nuclei contact each other**. Confocal microscopy analysis (A) and 3D reconstruction (B) revealed that tail-less nuclei (white arrow), tailed nuclei (green arrow) and lobed nuclei (yellow arrow) contact each other. Scale bar: 10 µm.

FIGURE 1

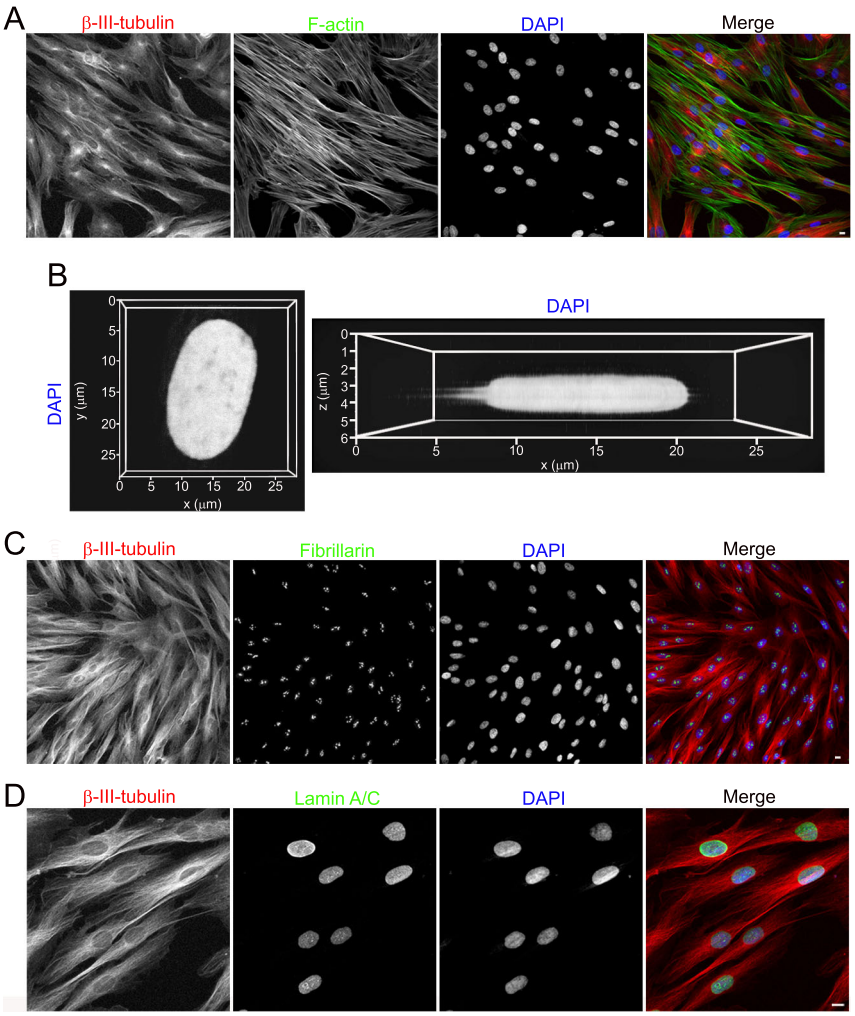
A
β-III-tubulin
F-actin
DAPI
Merge
B
DAPI
y (µm)
x (µm)
DAPI
z (µm)
x (µm)
C
β-III-tubulin
Fibrillarin
DAPI
Merge
D
β-III-tubulin
Lamin A/C
DAPI
Merge

FIGURE 2

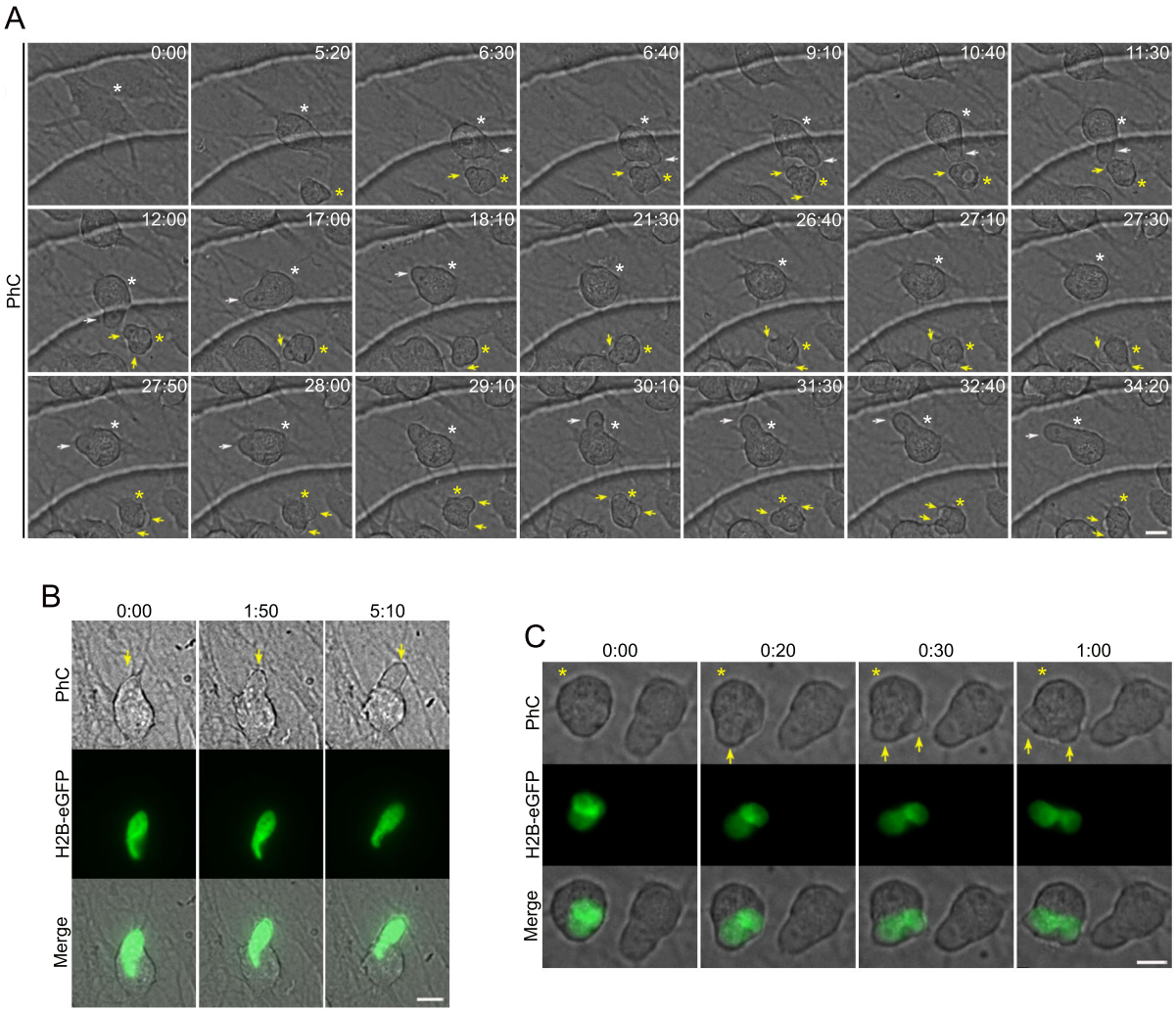
A
PhC
0:00
5:20
6:30
6:40
9:10
10:40
11:30
12:00
17:00
18:10
21:30
26:40
27:10
27:30
27:50
28:00
29:10
30:10
31:30
32:40
34:20
B
0:00
1:50
5:10
PhC
H2B-eGFP
Merge
C
0:00
0:20
0:30
1:00
PhC
H2B-eGFP
Merge

FIGURE 3

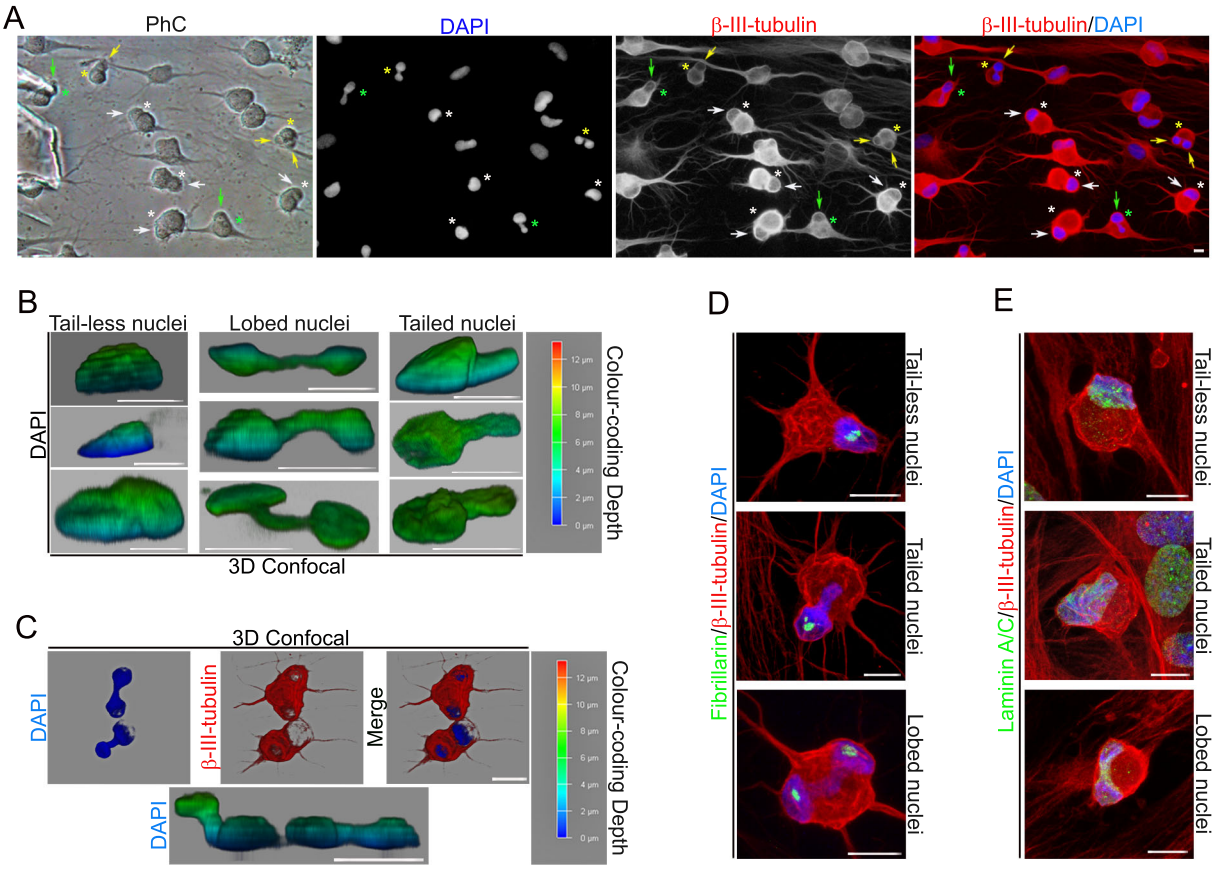
A
PhC
DAPI
β-III-tubulin
β-III-tubulin/DAPI
B
Tail-less nuclei
Lobed nuclei
Tailed nuclei
DAPI
3D Confocal
Colour-coding Depth
C
3D Confocal
DAPI
β-III-tubulin
Merge
DAPI
Colour-coding Depth
D
Fibrillarin/β-III-tubulin/DAPI
Tail-less nuclei
Tailed nuclei
Lobed nuclei
E
Laminin A/C/β-III-tubulin/DAPI
Tail-less nuclei
Tailed nuclei
Lobed nuclei

FIGURE 4

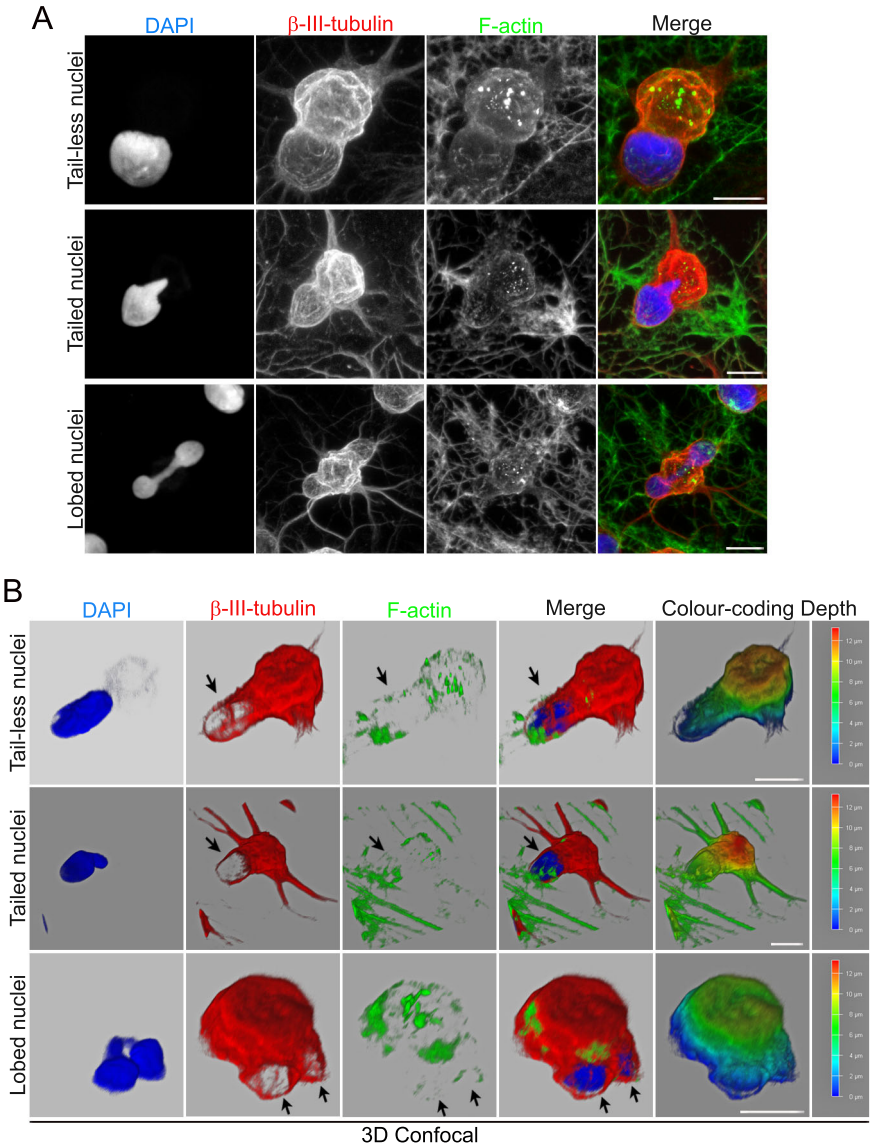
A
DAPI
β-III-tubulin
F-actin
Merge
Tail-less nuclei
Tailed nuclei
Lobed nuclei
B
DAPI
β-III-tubulin
F-actin
Merge
Colour-coding Depth
Tail-less nuclei
Tailed nuclei
Lobed nuclei
3D Confocal

FIGURE 5

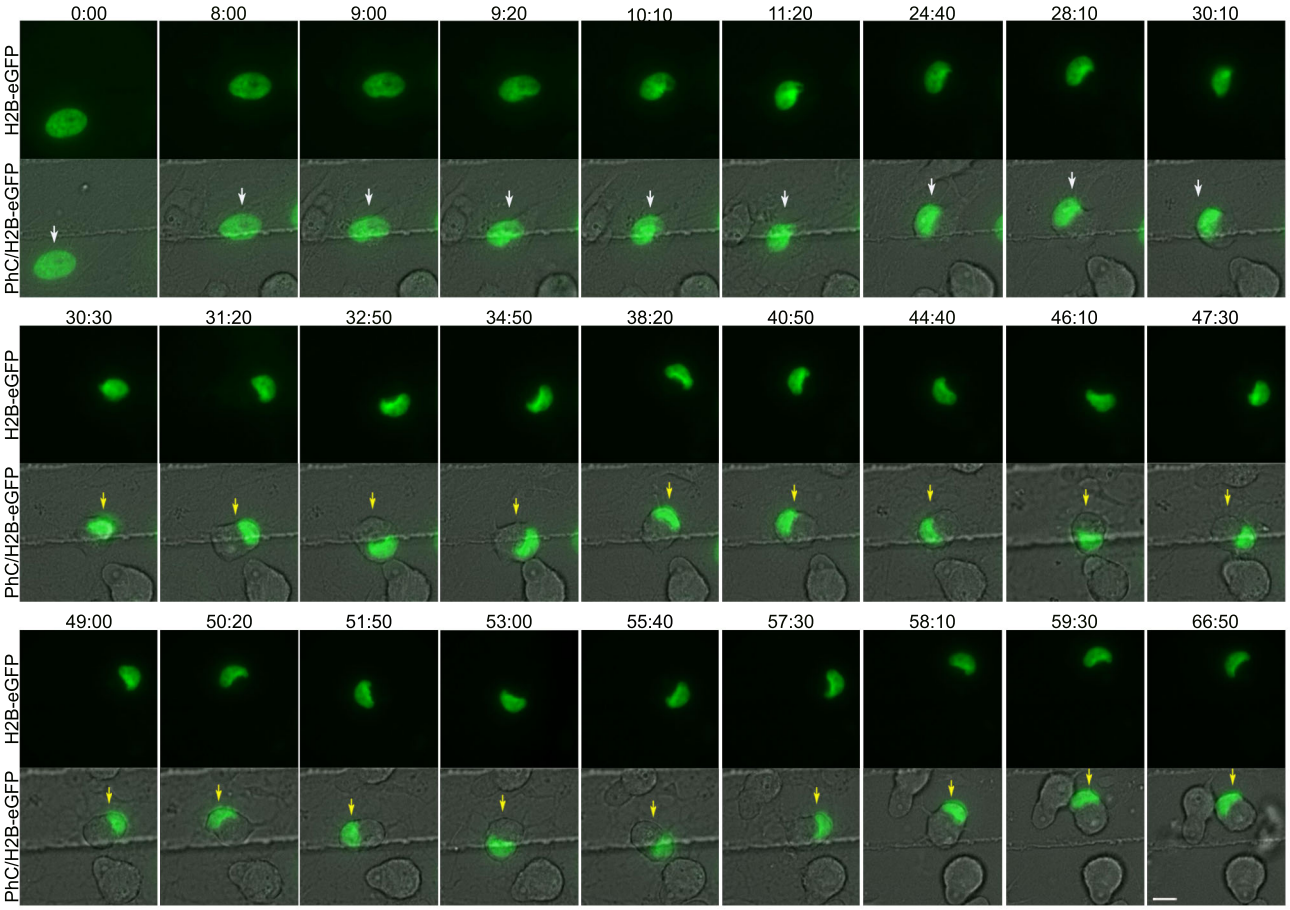
0:00
8:00
9:00
9:20
10:10
11:20
24:40
28:10
30:10
30:30
31:20
32:50
34:50
38:20
40:50
44:40
46:10
47:30
49:00
50:20
51:50
53:00
55:40
57:30
58:10
59:30
66:50
H2B-eGFP
PhC/H2B-eGFP

FIGURE 6

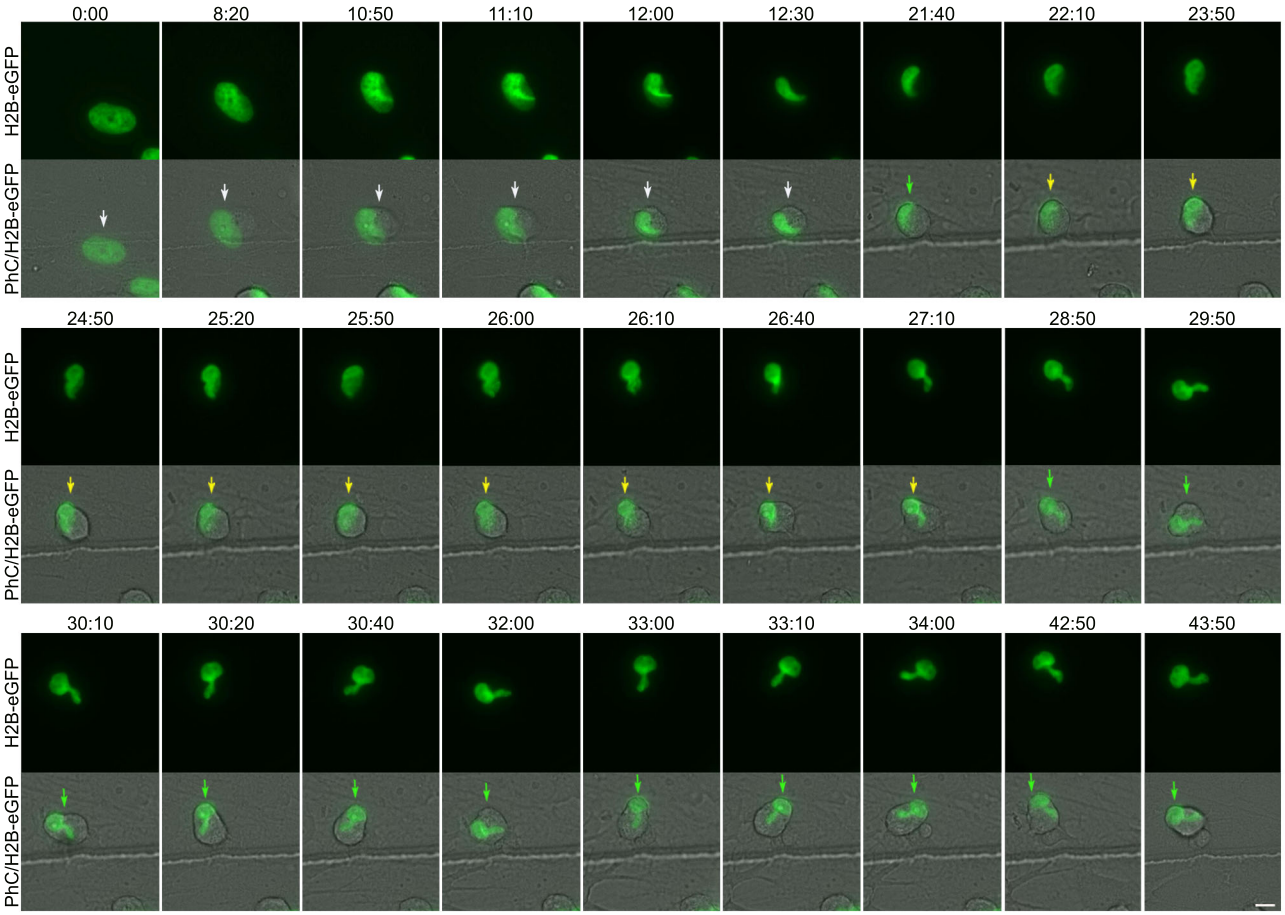
0:00
8:20
10:50
11:10
12:00
12:30
21:40
22:10
23:50
24:50
25:20
25:50
26:00
26:10
26:40
27:10
28:50
29:50
30:10
30:20
30:40
32:00
33:00
33:10
34:00
42:50
43:50
H2B-eGFP
PhC/H2B-eGFP

FIGURE 7

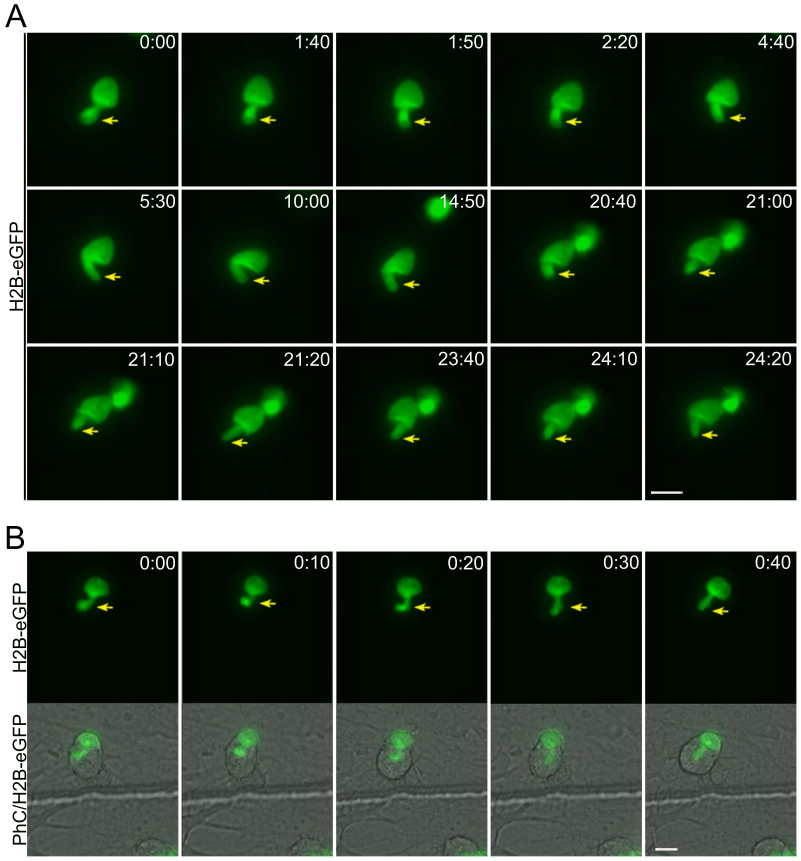
A
H2B-eGFP
0:00
1:40
1:50
2:20
4:40
5:30
10:00
14:50
20:40
21:00
21:10
21:20
23:40
24:10
24:20
B
H2B-eGFP
PhC/H2B-eGFP
0:00
0:10
0:20
0:30
0:40

FIGURE 8

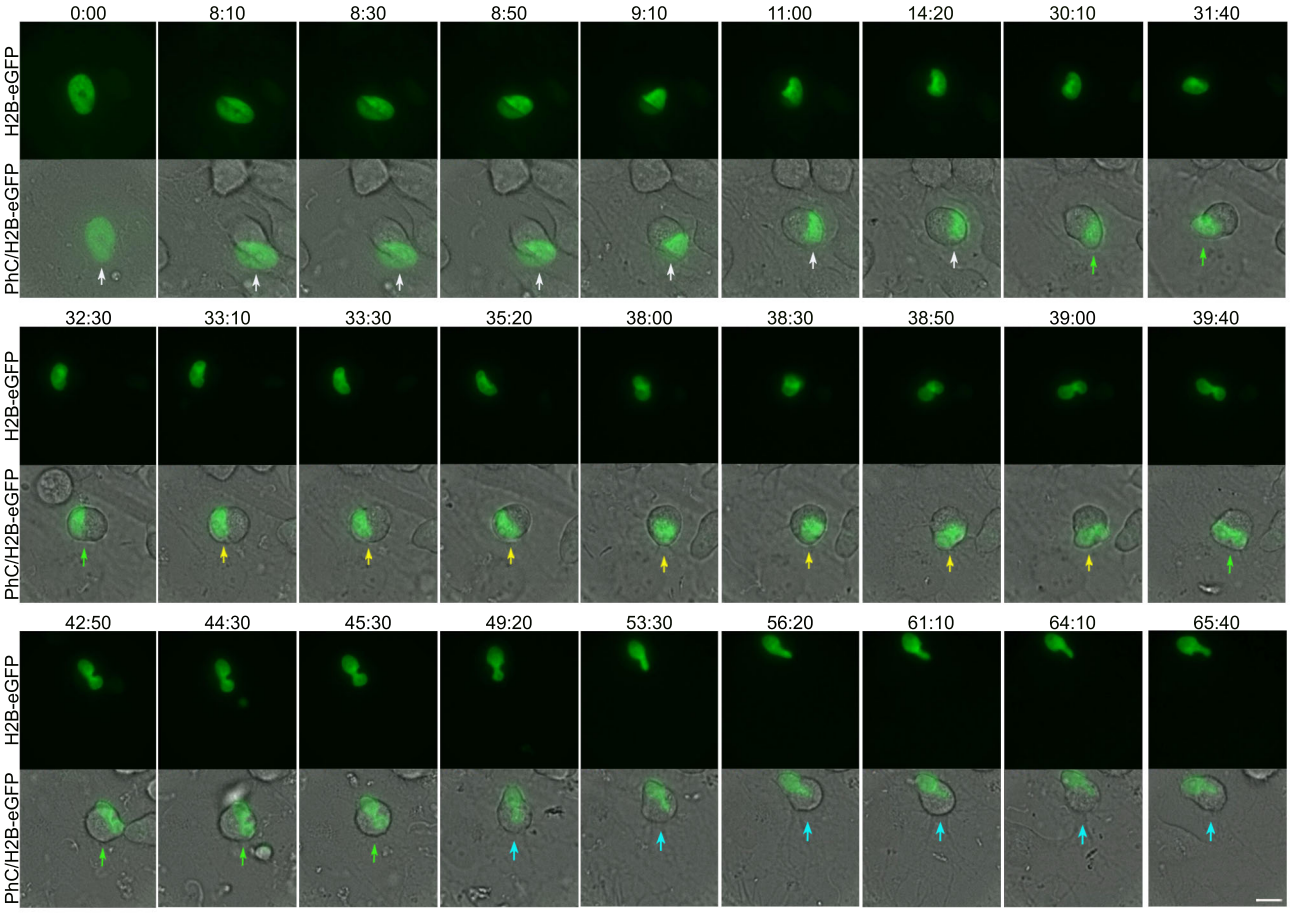
0:00
8:10
8:30
8:50
9:10
11:00
14:20
30:10
31:40
32:30
33:10
33:30
35:20
38:00
38:30
38:50
39:00
39:40
42:50
44:30
45:30
49:20
53:30
56:20
61:10
64:10
65:40
H2B-eGFP
PhC/H2B-eGFP

FIGURE 9

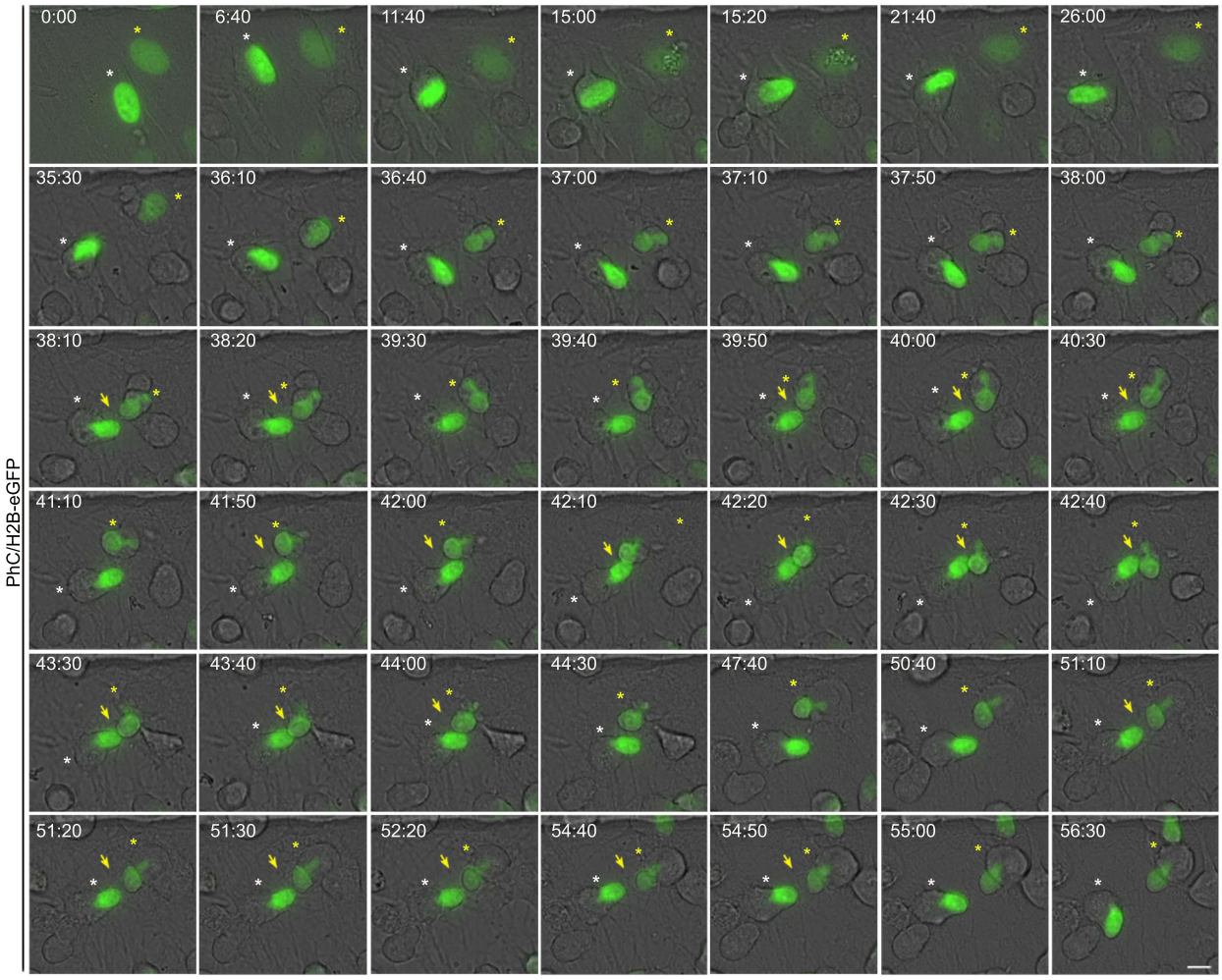
PhC/H2B-eGFP
0:00
6:40
11:40
15:00
15:20
21:40
26:00
35:30
36:10
36:40
37:00
37:10
37:50
38:00
38:10
38:20
39:30
39:40
39:50
40:00
40:30
41:10
41:50
42:00
42:10
42:20
42:30
42:40
43:30
43:40
44:00
44:30
47:40
50:40
51:10
51:20
51:30
52:20
54:40
54:50
55:00
56:30

FIGURE 10

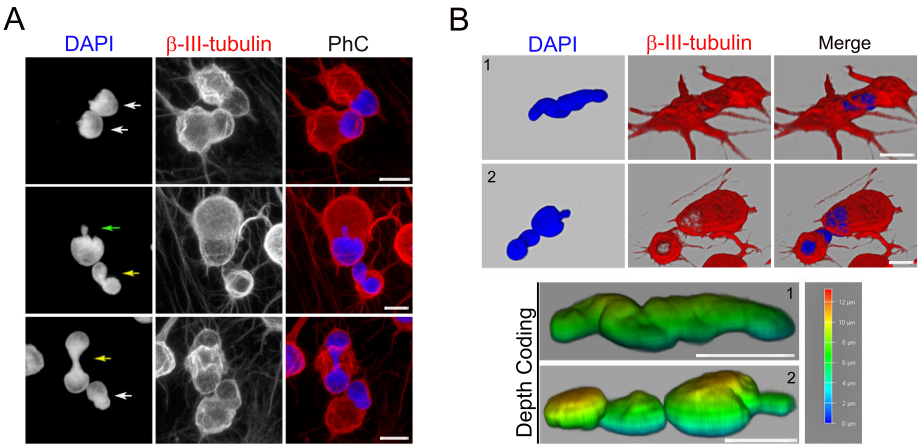
A
DAPI
β-III-tubulin
PhC
B
DAPI
β-III-tubulin
Merge
1
2
Depth Coding
1
2